



2025 Volume 33

Issue 4 Pages 389-399

https://doi.org/10.3846/jeelm.2025.25195

# MODELING SOIL RETENTION, EROSION POTENTIAL, AND SEDIMENTATION RISK USING THE INVEST SDR MODEL

Fatemeh MOHAMMADYARI<sup>1™</sup>, Khodayar ABDOLLAHI<sup>2</sup>, Mohsen TAVAKOLI<sup>3</sup>, Rosita BIRVYDIENĖ<sup>4</sup>

#### **Highlights:**

- forests retain 60% of watershed sediment, crucial for ecosystem health;
- innovative policies enhance soil conservation and sustainability;
- InVEST & SDR models support integrated watershed management;
- conservation principles guide land use policies for sustainability.

#### **Article History:**

- received 27 June 2024
- accepted 17 June 2025

**Abstract.** This study conducts an examination of the llam watershed, utilizing the InVEST and SDR models to assess soil retention, erosion, and transport. It incorporates factors like rainfall erosivity, soil erodibility, DEM, land use, vegetation, and conservation practices to explore the complex interplay between ecosystem services (ES) and disservices. The study found that the average soil retention in the watershed is 94.5 tons/ha/year, the average erosion potential is 62.8 tons/ha/year, and the average sediment transport is 10.5 tons/ha/year. Forest areas retain a significant portion of sediment (60%) with low discharge (13%), while agricultural and urban regions contribute more to erosion. This highlights the importance of integrating ES into land management strategies to mitigate environmental degradation. The study highlights the crucial role of ES in maintaining ecological balance and supporting human well-being. It advocates for innovative policies and customized solutions to mitigate land use impacts on soil conservation and sediment retention, thereby fostering awareness among managers and decision-makers for more sustainable land use planning.

Keywords: ecosystem services, environmental sustainability, soil retention, soil erosion, sedimentation, InVEST SDR.

#### 1. Introduction

Ecosystem services (ES) are the diverse benefits that humans derive, both directly and indirectly, from ecosystems (Yang et al., 2023a). The Millennium Ecosystem Assessment (2005) categorizes these services into four types: provisioning, regulating, cultural, and supporting. The first three categories have direct implications for human well-being and environmental integrity, whereas supporting services, though not directly beneficial to humans, underpin the other services by maintaining essential ecological structures and processes (Potschin-Young et al., 2017). Conversely, the negative impacts on ecological, environmental, and human systems resulting from the loss of these services are termed "ecosystem damages or disservices." These damages often manifest as dysfunctional ecosystem functions that adversely affect human welfare (Paudel & States, 2023).

Ecosystem damages or disservices can be defined as the detrimental effects that arise when ecosystem functions are impaired or lost, leading to negative consequences for both the environment and human communities. Understanding both ES and damages is crucial for informed decision-making. It also helps mitigate misinformation (Carucci et al., 2022). Soil conservation is a regulatory service that mitigates soil erosion through the ecosystem's capacity to retain soil (Srichaichana et al., 2020). Soil erosion is a significant global environmental challenge, driven by the detachment, transport, and deposition of soil particles by agents such as water, wind, and gravity (Gadisa & Midega, 2021). The interaction of natural factors—like rainfall, topography, and soil characteristics with human activities—such as agriculture, deforestation, and urbanization—exacerbates soil loss and sediment transport, negatively impacting ES and functions (Degife

<sup>&</sup>lt;sup>1</sup>Department of Environmental Engineering, Faculty of Natural Resources and Earth Sciences, Shahrekord University, Shahrekord, Iran

<sup>&</sup>lt;sup>2</sup>Department of Nature Engineering Faculty of Natural Resources and Earth Sciences, Shahrekord University, Shahrekord, Iran

<sup>&</sup>lt;sup>3</sup>Department of Rangeland and Watershed Management, Faculty of Agricultural, Ilam University, Ilam, Iran

<sup>&</sup>lt;sup>4</sup>Department of Geodesy and Cadaster, Vilnius Gediminas Technical University, Vilnius, Lithuania

<sup>&</sup>lt;sup>™</sup>Corresponding author. E-mail: *mohammadyari.f@sku.ac.ir* 

et al., 2021; Yohannes et al., 2021). As a form of ecosystem damage, soil erosion leads to numerous problems, including environmental degradation (Borrelli et al., 2017), socio-economic issues (Tamire et al., 2022), desertification (Guo et al., 2022), land degradation, food security concerns (Balabathina et al., 2020), climate change, and mass human migration (Getu et al., 2022).

In Iran, soil erosion rates are estimated at approximately 50 tons per hectare annually, with an increase of 10 tons per hectare over the past decade. This erosion rate corresponds to a yearly reduction of one millimeter in soil thickness nationwide (Sadat et al., 2023). Consequently, quantifying sediment retention and assessing erosion and sedimentation potential are critical for policymakers and planners (Hamel et al., 2015). Sediment transport refers to the process by which sediment is moved from its source to a destination, often involving water or wind as the transporting medium. Sediment transport is a critical component of the erosion process, as it involves the detachment and movement of soil particles. While sediment delivery specifically refers to the proportion of sediment that is actually delivered to a water body or other sink, as opposed to being retained within the landscape. Sediment delivery is an important metric for assessing the impact of erosion on water quality and ecosystem health. The Universal Soil Loss Equation (USLE) was the initial method for evaluating soil erosion. It was later refined into the Revised Universal Soil Loss Equation (RUSLE) to enhance its applicability across various conditions. However, these models do not account for sediment transport to water bodies. To address this gap, the InVEST SDR model was developed by Stanford University's Natural Capital Project, enabling the estimation of soil loss, sediment transport, sediment retention, and other erosion-related components (Tamire et al., 2022). The InVEST SDR model's application in sediment retention modeling and erosion potential estimation has been validated in numerous studies. The modeling of soil retention and the estimation of erosion potential using the InVEST SDR model have been the focus of numerous studies, and the capabilities of this model for mapping and output generation have been validated. Examples of international studies in this field include the identification of land use change impacts on sediment transport in the Qiantang River basin, China (Zhou et al., 2019), the assessment of soil loss and sediment transport in the Nile basin watershed, Ethiopia (Gashaw et al., 2021), the evaluation of land use changes on soil erosion in the Rio da Prata basin, Brazil (da Cunha et al., 2022), the estimation of soil loss and mapping of intensity in the Megch watershed, Ethiopia (Getu et al., 2022), the assessment of ES based on land use simulation: a case study in the Heihe River basin, China (Zhao et al., 2022), the quantification of soil retention changes to identify priority conservation areas in Qinghai (Liu et al., 2023), the examination of soil retention changes in the tropical regions of southwestern China (Yang et al., 2023b), and the modeling of soil erosion sensitivity including sediment connectivity and transport at the landscape scale using InVEST-SDR and Fragstats (Bhattacharya et al., 2024).

Both the MUSLE and the InVEST SDR model are widely used for assessing soil erosion and sediment transport. Unlike the USLE and its revised version (RUSLE), which primarily focus on soil erosion, MUSLE and InVEST SDR models incorporate sediment yield and transport into their calculations. This makes them particularly suitable for studies aiming to evaluate erosion risk and sedimentation impacts. MUSLE is an extension of USLE that incorporates runoff energy to estimate sediment yield more accurately. It is beneficial in scenarios where runoff data is readily available and can provide detailed insights into the sediment transport process. MUSLE requires specific runoff data, which might not always be available, limiting its applicability in areas with sparse hydrological data. The InVEST SDR model combines the RUSLE equation with a sediment delivery ratio to estimate sediment export. It is advantageous in large-scale watershed assessments where detailed spatial analysis of sediment transport is crucial. It also integrates well with GIS data, allowing for comprehensive spatial mapping of erosion and sedimentation risks. While effective for large-scale assessments, InVEST SDR may not provide the same level of detail on runoff dynamics as MUSLE. For this study, the InVEST SDR model was chosen due to its ability to provide spatially explicit results, which are essential for identifying high-risk erosion areas and planning targeted conservation efforts. Additionally, its integration with GIS data facilitates a more comprehensive analysis of watershed dynamics.

Given the underrepresentation of the multi-purpose value of ecosystems and the concept of ecosystem damage in scientific literature, this study aims to evaluate ecosystem processes in the llam watershed to enhance soil conservation and manage flood and sediment risks. This is achieved through the spatial modeling of sediment retention as an ecosystem service and erosion and sedimentation as ecosystem damages using the InVEST SDR model. Addressing soil fertility reduction due to soil erosion is a critical ecological concern.

# 2. Materials and methods

# 2.1. Description of the study area

The llam watershed, situated in the northern region of llam province, spans from 46°18′ to 46°30′ east longitude and from 33°34′ to 33°41′ north latitude. The watershed encompasses an area of 13,185 hectares with an elevation range of 1139 to 2461 meters above mean sea level (MSL). This variability in elevation significantly influences the hydrological processes and sediment transport dynamics within the basin. Additionally, the basin's slope, which ranges from 0.0016 to 47%, plays a crucial role in assessing erosion risk. Steeper slopes are more prone to erosion due to increased runoff velocity and energy, while gentler slopes may experience less erosion but could still contribute significantly to sedimentation due to longer flow paths and potential deposition areas. Land cover is predominantly forested (52%), urbanized

(24%), with agricultural land comprising 14%, pastures 3%, gardens 2%, rivers 2%, roads 2%, and parks less than 1%. The remaining land use categories, including other minor features, account for the balance to ensure that the total percentage equals 100% (Figure 1). The prevalent soil texture within the watershed is sandyloam. Erosion manifests in various forms, including surface erosion, rills, gullies, spillways, and channels. The soil texture within the watershed is predominantly sandy-loam, with variations across different sub-basins. Sandy-loam soils are characterized by a mix of sand, silt, and clay, which influences their erodibility and water retention capacity. The distribution of soil types across the watershed is as follows:

- Sandy-Loam Soils: These are the most prevalent, covering approximately 65.2% of the watershed. They are relatively susceptible to erosion due to their high sand content but also allow for good drainage, which can mitigate runoff-induced erosion.
- Loam Soils: Found in about 6.61% of the area, these soils have a relatively high resistance to water erosion due to their balanced composition of sand, silt, and clay. These soils retain moisture well and provide relatively good drainage, which prevents the rapid leaching of nutrients. Additionally, their porous structure facilitates aeration and water retention, helping to mitigate the effects of erosion.
- Other Soil Types: The remaining 28.19% includes a mix of clay, sand, and other minor soil types, each

with unique characteristics affecting their erosion potential. Overall, while clay-loam-sandy soils have some resistance to erosion due to their structure, they can still be vulnerable under certain conditions, especially when exposed to heavy rainfall or strong winds. Proper management practices and maintaining vegetation cover are essential for minimizing erosion risks.

Geologically, the watershed features a mix of sedimentary and metamorphic rocks, which influence soil formation and erosion susceptibility. Historically, the area has experienced significant erosion, particularly during heavy rainfall events, exacerbated by factors such as low canopy cover and a semi-humid climate with high precipitation. The basin's vulnerability to erosion is further highlighted by the presence of surface erosion, rills, gullies, spillways, and channels, underscoring the need for targeted conservation strategies. The basin's vulnerability to erosion is exacerbated by factors such as low canopy cover across different land uses, a semi-humid climate with high precipitation, and the geological formations' inherent sensitivity. Consequently, land use, climate, geology, and land cover are identified as the primary drivers of erosion occurrence and intensification within the watershed. The Ilam watershed is further divided into twelve sub-basins, namely West Ban Jo (code 1), Saleh Abad Road (code 2), Ban Jo (code 3), East Ban Jo (code 4), Chalimar (code 5), Milad Square (code 6), Kaleh Anar (code 7), Arghvan (code 8), MianHoza (code 9), East city Ilam (code 10), North Choghasbez (code 11), and Mahdi Abad (code 12).

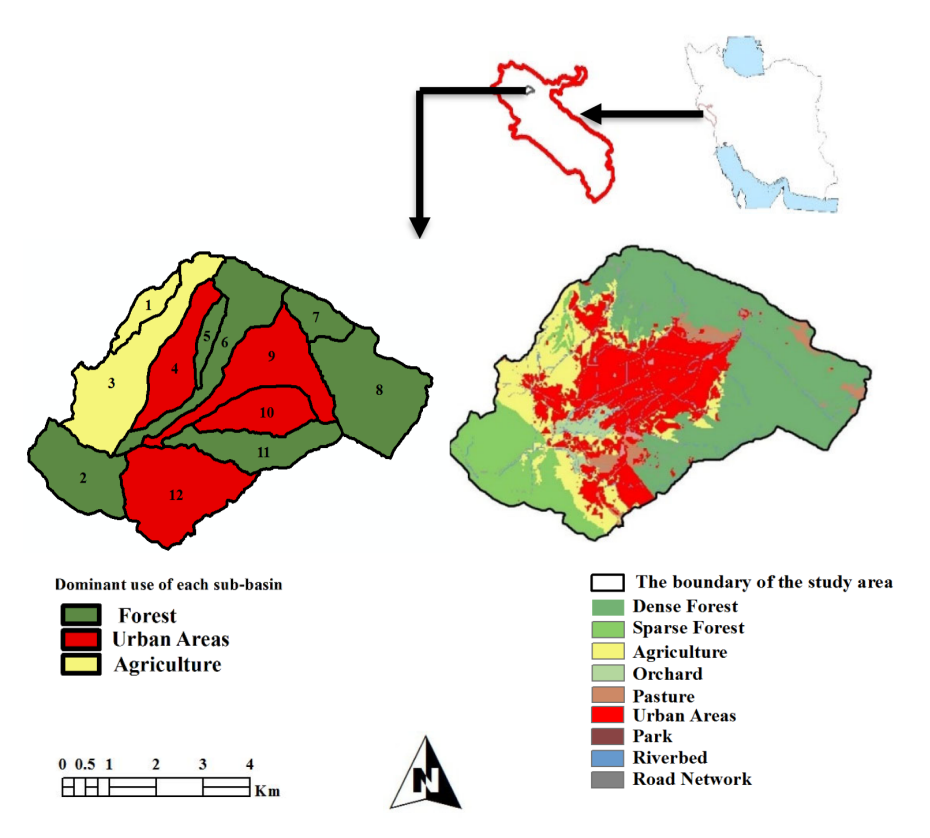


Figure 1. Geographical location of Ilam Watershed and its land cover distribution

A Digital Elevation Model (DEM) was obtained from NASA's Shuttle Radar Topography Mission (SRTM)to support terrain analysis in the study. Twenty years of rainfall data were collected from five rain gauge stations across the study area. These data were used to calculate the rainfall erosivity factor (R factor), which is essential for estimating soil erosion potential. Land use/land cover maps were obtained from satellite imagery. These maps were used to assign crop management (C) and support practice (P) factors, which reflect the impact of land use practices on soil erosion. Soil maps were sourced from FAO's maps. These maps provided the necessary information to determine the soil erodibility factor (K factor), which varies based on soil type and composition. Preprocessing steps included ensuring all data were in a compatible format and resolution for the InVEST SDR model. The DEM was used to derive slope and flow direction rasters, while rainfall data were processed to calculate the R factor using established methods.

The meteorological data used in this study were collected from 28 stations located within and around the llam watershed. The data collection involved recording monthly

**Table 1.** Characteristics and geographic locations of rain gauge stations used in the study

Station name	Х	Υ	Precipitation (mm)	R factor	
	725825	3652033	588.6	302.9	
Abdanan	703786	3662645	531.9	259	
	770555	3612463	380.38	157.14	
	621330	3661276	612.41	322.29	
	626092 3653944 250.56		250.56	87.59	
Mehran	643109	3661570	258.96	91.6	
Ivieman	658366	3680290	497.94	234.27	
	602097	3714652	328.43	127.34	
	651952	3693128	471.17	215.52	
	611294	3722127	376.25	154.67	
llam	611165	3733235	466.63	212.41	
	584851	3740354	384.61	159.71	
Sirvan	674912	3710154	400.56	169.42	
Chardaval	722134	3744418	423.44	183.83	
	651282	2 3735635 434.81		191.18	
	632550	3750144	534	260.8	
Eyvan	618609	3755505	599.18	311.47	
	598525	3760820	517.56	245.45	
Darrehshahr	738062	3661569	442.9	196.48	
Darrensnam	760195	3649183	464.48	210.94	
	706113	3625713	299.2	77.72	
	747865	3580431	179.68	56.55	
	776012	3584863	277.21	76.82	
Dehloran	678856	3664007	419.79	181.5	
Denioran	688898	3627219	253	88.79	
	691985	3629127	302.14	113.26	
	669939	3639816	281.27	102.56	
	723874	3600210	233.15	79.51	

and annual precipitation amounts over a 23-year period (Table 1). The data were obtained using standard rain gauges and were analyzed using the Kriging interpolation method in a GIS environment to ensure spatially representative rainfall erosivity factors. This approach allowed us to accurately assess the climatic conditions influencing soil erosion and sediment transport in the study area.

## 2.2. Modeling approach

Understanding sediment dynamics is crucial for local environmental management, prompting the development of tools with varying complexity levels. One challenge in model integration is accurately predicting sediment deposition on terrestrial surfaces or within streams and pinpointing the sources of sediment. In data-scarce scenarios, simplified tools are employed to evaluate ecosystem services, focusing on the trade-offs and synergies among services under different land-use and climate conditions (Hamel et al., 2015). In response to this need, the InVEST software suite includes a sediment retention model that aligns with this philosophy, assessing the capacity of watersheds to retain soil within the landscape (Kusi et al., 2020). In this study, the InVEST SDR model was utilized, taking into account various input variables such as Borselli parameters, DEM, rainfall erosivity factors, maximum sediment delivery ratio, and biophysical parameters. The Revised Universal Soil Loss Equation (RUSLE) was used as shown in Equation (1). The RUSLE model, known for its cost-effectiveness and minimal data requirements, facilitates the spatial analysis of soil loss patterns (Getu et al., 2022; Azimi Sardari et al., 2019), enabling the identification of critical areas contributing significantly to soil depletion.

$$RUSLE_{i} = (R.K.LS.P)_{i}, (1)$$

where *RUSLE* means annual soil loss (t ha<sup>-1</sup> year<sup>-1</sup>), *K* indicates the soil erodibility Mg h ha<sup>-1</sup> MJ<sup>-1</sup> mm<sup>-1</sup>, *R* indicates the rainfall erosivity factor, denoted as MJ mm ha<sup>-1</sup> h<sup>-1</sup> yr<sup>-1</sup>, which is a climatic parameter aiding soil loss through the detachment and transport forces of raindrop impact and runoff (Getu et al., 2022). This factor is determined by soil stripping, erosion, and removal parameters as follows (Bhattacharya et al., 2024):

$$R = \sum_{i=1}^{12} 1.35 \times 10^{\left[1.5 \log \left(\frac{P^2}{P_{tot}} 0.8188\right)\right]},$$
 (2)

where P is the average monthly precipitation (mm) and  $P_{tot}$  is the average annual precipitation (mm). This parameter was prepared based on monthly and annual precipitation data from meteorological stations over a 30-year period using the Kriging interpolation method in a GIS environment. K is soil erodibility factor, represented in Mg h MJ<sup>-1</sup> mm<sup>-1</sup>, reflects the inherent sensitivity of soil to erosion by water, rain, and runoff (Ougougdal et al., 2020; Mazigh et al., 2022). It essentially indicates the soil's susceptibility to removal by surface flow (Degife et al., 2021). In the current research, 9 soil profiles were exca-

vated during field visits, and soil samples from 22 horizons were collected for laboratory analysis to measure the desired parameters). The Modified Pacific Southwest Inter-Agency Committee (MPSIAC) model is an adaptation of the original PSIAC model, developed in 1982 to improve sediment yield predictions by incorporating additional factors. It utilizes nine effective factors influencing erosion and sediment production, including surface geology, soil type, climate, runoff, topography, ground cover, land use, upland erosion, and channel erosion. The MPSIAC model estimates long-term average annual erosion rates and has been successfully applied in various semi-arid regions (Zakeri et al., 2015). For further details on its functionality and applications, see Sadeghi (1993), which discusses modifications made to the original PSIAC model. The K factor for the sub-basins of the watershed was then determined based on the MPSIAC model (Equation 3) and the Wischmeier nomograph, considering soil structure, infiltration rate, organic matter percentage, and soil texture (percentage of sand, silt plus very fine sand.

$$Y = 16.67 X,$$
 (3)

where Y is the soil erodibility factor, and X is the soil erodibility factor derived from the Universal Soil Loss Equation by Wischmeier and Smith. The K value for soil units was determined based on the percentage of silt, very fine gravel, sand, organic materials, structure, and permeability of the soil. Ultimately, these values were finalized according to the InVEST SDR model guide (Sharp et al., 2020) and based on the texture and organic matter information of the soil in the region for each soil category, and a checkerboard map of this factor was produced in a GIS environment. LS was shown to be influenced by the topography, which is determined by both the length and steepness of the slope. The highest Slope Length-Steepness Factor (LS) values are typically found in areas with high slopes, such as dissected highlands or isolated hillocks on the edges of plateaus, while the lowest values are observed on flat surfaces or lowlands (Bhattacharya et al., 2024). C (dimensionless) refers to the type of land cover and use, indicating the trend of sensitivity to natural and human activities (Liu et al., 2021). The Normalized Difference Vegetation Index (NDVI) is a widely used remote sensing method for assessing vegetation health and density, calculated based on the near-infrared and red spectral bands. In this study, NDVI values were derived from Sentinel-2 satellite imagery, which provides multispectral data critical for vegetation analysis. Pre-processing steps included cloud removal to eliminate atmospheric interferences and geometric corrections to align imagery accurately. NDVI was calculated by applying the formula to the relevant bands of the satellite data. The resulting NDVI values, ranging from -1 to 1, were visualized using color gradients to highlight areas of varying vegetation health. These NDVI values were then used to define the cover management factor (C factor) in soil erosion modeling, as they represent the effect of vegetation cover on soil erosion rates. By incorporating NDVI into the analysis, we ensured accurate representation of vegetation conditions, which is essential for estimating sediment retention and erosion potential in the study area. This factor was calculated based on the following equation (Getu et al., 2022; Liu et al., 2021):

$$C = (1 - NDVI/2). \tag{4}$$

Our rainfall erosivity analysis utilized 28 years of meteorological data (1995–2022) to account for long-term climatic variability, while vegetation cover was assessed using imagery from 2022. This methodological distinction was based on the R factor's need for multi-decadal precipitation data, whereas NDVI from a single recent year offers a reliable snapshot of contemporary land cover conditions. The selected dataset provided detailed vegetation insights, supported by the availability of cloud-free composite images. Although multi-year NDVI data could reveal vegetation dynamics, we prioritized consistency by aligning the 2022 NDVI data with land use classifications from the same year, ensuring coherence in C factor calculations for soil erosion modeling.

P (dimensionless) is a factor measuring soil conservation. The values of this factor were determined through the reclassification of land cover types (Moges & Bhat, 2017; Gashaw et al., 2018; Getu et al., 2022) and based on a literature review (Getu et al., 2022; Sadat et al., 2023) (Table 2). Generally, the numerical range of this factor is 1 for soils without conservation practices and approaches zero when appropriate erosion control measures are implemented (Ganasri & Ramesh, 2016; Mazigh et al., 2022; Getu et al., 2022).

Table 2. p value for land use and land cover

Land use	Value		
Forest	0.8		
Agriculture	0.5		
Orchard	0.1		
Pasture	0.7		
Urban Areas	0.9		
Park	0.7		
Riverbed	1		
Road Network	1		

Sediment delivery ratio (SDR) elucidates the link between where sediments come from and where they end up, considering how sediment detachment and transport are closely related. This connection is influenced by upslope  $D_{up}$  and downslope  $D_{up}$  factors, which are determined by the land use and topography within a specific watershed (Equation 5).

$$IC = \log_{10} \left( \frac{D_{up}}{D_{dn}} \right), \tag{5}$$

where  $D_{up}$  is the upslope component defined by Equation (6):

$$D_{up} = \overline{\mathsf{CS}}\sqrt{\mathsf{A}},\tag{6}$$

where  $\overline{C}$  is the average weight coefficient (dimensionless),  $\overline{S}$  is the average slope gradient in the upslope region (m/m), and A is the area of the upslope region (m<sup>2</sup>).

The  $D_{dn}$  component reflects the sediment transport potential along the flow path to definite sink points, depending on Land Use Land Cover (LULC), slope gradient, flow path, and flow distance.  $D_{dn}$  can be expressed as:

$$D_{dn} = \sum_{i} \frac{d_i}{w_i S_i},\tag{7}$$

where  $d_i$  is the flow path length along pixel i (m) so it effectively indicates the average length of the flow path in the downslope direction for each pixel within the watershed model,  $w_i$  represents the average weight coefficient of cell i (dimensionless), and  $S_i$  denotes the average slope of cell i (m/m). Subsequently, the *SDR* ratio for pixel i was derived from the connectivity index *IC* based on Equation (8) (Sharp et al., 2020).

$$SDR_{i} = \frac{SDR_{\text{max}}}{1 + \exp\left(\frac{IC_{0} - IC_{i}}{k}\right)},$$
(8)

where  $SDR_{max}$  is the theoretical maximum SDR set to an average value of 0.8. Additionally, the parameters  $IC_0$  and k

are calibrated using the values of 0.5 and 2, respectively, as suggested by Vigiak et al. (2012) and Hamel et al. (2015).

A DEM in this study with a 30-meter resolution was utilized. The land use map for the year 2022 was extracted from the Landsat satellite's OLI sensor imagery. Following necessary pre-processing and geometric and atmospheric corrections, the image was classified using the Support Vector Machine algorithm into 9 land use categories including dense and sparse forests, agriculture, orchards, pastures, urban areas, parks, rivers, and roads. The Kappa coefficient of the image was 96 percent, confirming the high accuracy and validity of the land use map. It is noteworthy that a biophysical table in CSV format containing land use codes, cover management factors, and conservation practice factors for each land use category was designed and utilized for the model execution.

### 3. Results

The spatial distribution of the conservation practice factor (P), soil erodibility factor (K), rainfall erosivity factor (R), slope length-gradient factor (LS), and cover management factor (C) is depicted in Figure 2.

Based on this, the soil erodibility factor in the Ilam watershed ranges from 0.14 to 0.34 Mg h ha<sup>-1</sup> MJ<sup>-1</sup> mm<sup>-1</sup>, with the highest values observed in urban areas. The

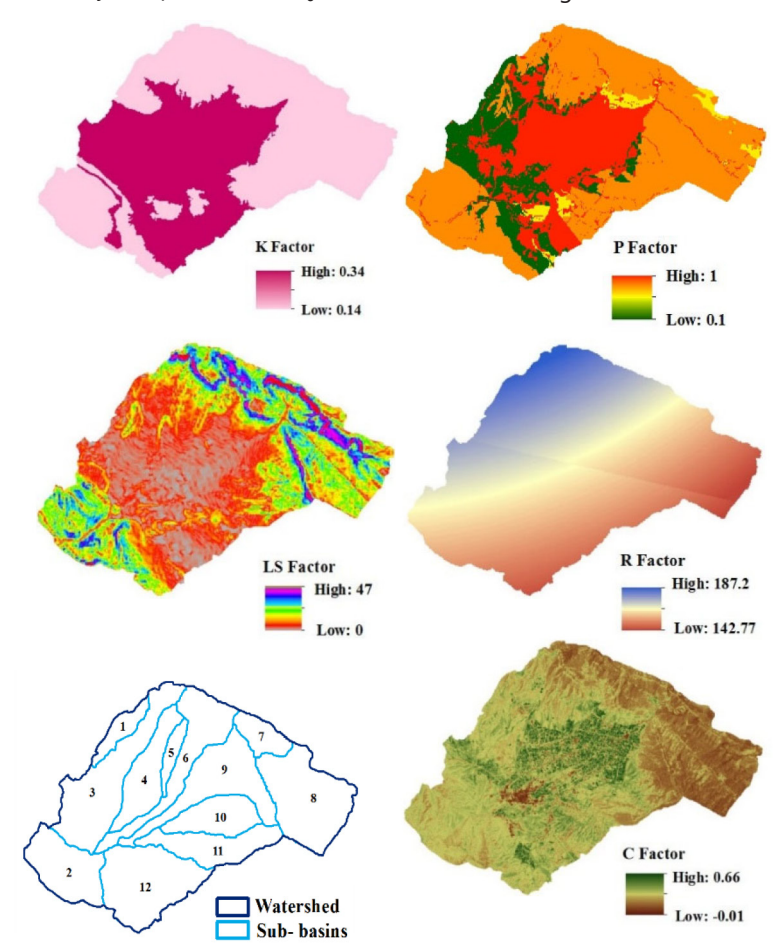


Figure 2. Input layers of the InVEST SDR model for the studied basin

conservation practice factor was set to 1, reflecting the infrequent implementation of conservation and management practices in the region. The slope length-gradient factor was determined to be between 0 and 47. Additionally, the rainfall erosivity factor values span a numerical range of 142 to 187 MJ mm ha<sup>-1</sup> h<sup>-1</sup>yr<sup>-1</sup>. Correspondingly, the cover management factor ranges from 0.01 to 0.66, with lower values indicating areas with vegetative cover and higher values denoting regions lacking vegetative cover. The model calibration process for the InVEST SDR model involved several key steps to improve predictions of sediment yield and retention by adjusting parameters such as the SDR, rainfall erosivity (R), soil erodibility (K), slope length-gradient (LS), and cover management factor (C). To evaluate sensitivity, a systematic sensitivity analysis was performed by varying key parameters such as connectivity index calibration parameter and k (scaling factor for SDR) to assess their impact on model outputs. The study also utilized a DEM with a 30-meter resolution and validated land use data with a Kappa coefficient of 96%, ensuring high accuracy. Following the implementation and calibration of the InVEST SDR model, the annual potential for erosion, sediment deposition, and soil retention was estimated at a pixel resolution of 30×30 meters for the sub-basins (refer to Figure 3 and Table 3). The potential for erosion varies from 0 to 155 tons per pixel. Conversely, the minimum and maximum sediment export values are respectively 0 and 40 tons per pixel. The annual soil retention capacity ranges numerically from 0 to 114.35 tons per pixel. In terms of spatial distribution, the central, southsouthwestern, and northwestern sections exhibit higher levels of soil erosion potential and sediment export, while the northern, eastern, and western regions, predominantly forested, play a significant role in soil retention.

Table 3. Final results of the InVEST SDR model

Sub- basin	Area	Soil retention	Erosion potential	Sediment transport		
Dasiii	ha	Tons/ha				
1	346	0.97 1.1 0.13				
2	1152	12.8	6	0.44		
3	1869	10	13.2	1.33		
4	938	2.2	11	1.44		
5	244	1.1	2.2	0.22		
6	1258	13.7	7.1	0.77		
7	441	9.8	2.1	0.22		
8	1840	24.9	4.4	0.33		
9	1509	7.2	2.7	2.6		
10	820	1.6	8.6	1		
11	978	4.29	2.65	0.2		
12	1790	6	1.77	1.77		
Total	13185	94.56	62.82	10.45		

According to the results presented in Table 3, the soil retention capacity for the entire watershed is estimated at 94.56 tons per hectare annually. Similarly, the annual erosion potential for the entire watershed is calculated to be 62.82 tons per hectare per year. Additionally, the sediment transport for the entire watershed amounts to 10.45 tons per hectare annually. As observed, Sub-basin 8 exhibits

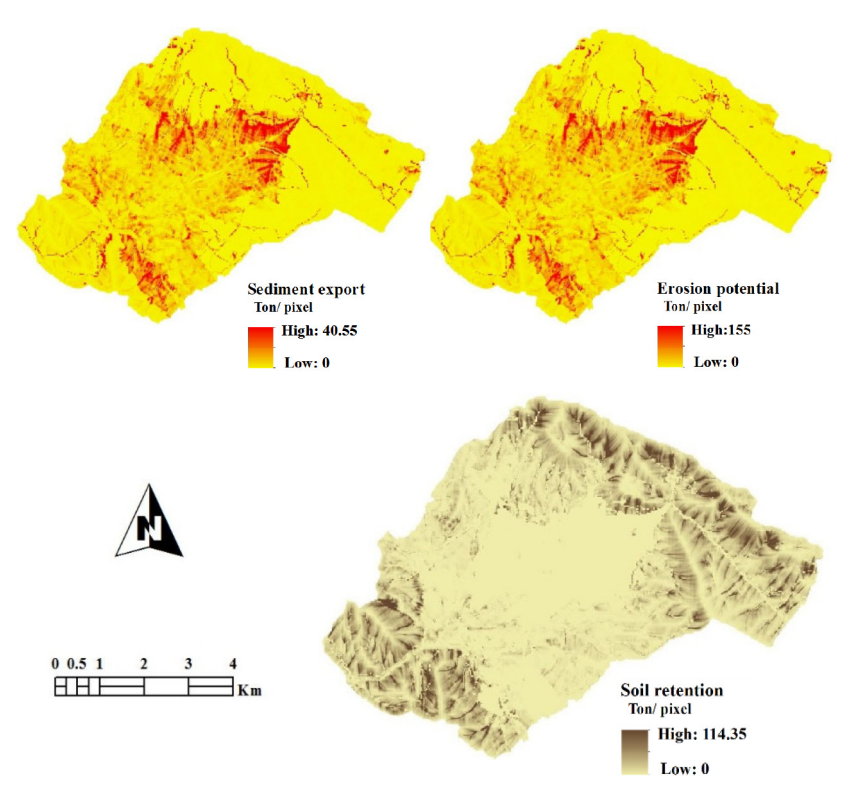


Figure 3. InVEST SDR model output maps for the basin of interest

the highest, and Sub-basin 1 the lowest, soil retention potential. The dominant land covers of these sub-basins are forest and agriculture use, respectively (Table 4).

**Table 4.** Soil retention capacity, erosion, and sedimentation associated with predominant land use within sub-basins

Land use	Sub-basin	Soil retention	Erosion potential	Sediment transport
		potential	Percentage	transport
Forest	2-5-6-7- 8-11	60	25	13
Agriculture	1-3	12	14	14
Urban Areas	4-9-10-12	18	61	73

Furthermore, the highest rates of erosion and sediment transport were recorded in Sub-basins 3 and 9. Agriculture and Urban areas constitute the predominant land cover in Sub-basins, respectively. In light of the findings in Table 3, sub-basins with a majority forest cover have allocated the greatest amount of soil retention, equivalent to 60 percent, and the least sediment transport, equivalent to 13 percent of the total watershed. Conversely, the lowest soil retention rate (12 percent) was observed in agricultural lands. On the other hand, sub-basins with predominantly urban areas have the highest erosion and sediment transport. Owing to the variability in soil retention capacity, as well as the potential for erosion and sedimentation across various land uses, the corresponding values are delineated individually for each category of land utilization in Table 5.

Future climate scenarios for the study area, based on IPCC projections, indicate that under RCP 4.5, temperatures could rise by 1.4 °C by 2050 with a 5–10% increase in precipitation, potentially intensifying rainfall erosivity by 15–20%. Under RCP 8.5, warming may reach 2.0 °C with more variable precipitation and up to a 30% increase in extreme rainfall events. Although overall precipitation changes may be modest, llam's semi-arid climate and topography make it sensitive to these shifts. To address these changes, the model framework can adapt by adjusting the R factor in RUSLE for rainfall intensity, modifying C factors for vegetation changes, and incorporating projected land

use changes, ensuring robust soil erosion predictions for llam under future climate and development scenarios.

## 4. Discussion

The spatial distribution of soil retention as an ES, and soil erosion and sediment transport as ecosystem disservices, are of great importance for sustainable land management and the development of appropriate conservation programs. In this regard, this study highlighted the dynamic process of soil loss using the InVEST SDR model to identify the sources of erosion and sediment transport, as well as soil retention in the Ilam watershed. The investigation of this process revealed patterns and distributions that vary significantly, with the potential for soil loss and sediment yield being more severe in the central and southern parts of the Ilam watershed compared to the northern, eastern, and western parts. This pattern is reversed for soil retention, where the northern, eastern, and western parts are prioritized for soil conservation due to forest cover (Figure 3). The canopy and deep roots of vegetation increase soil organic matter, subsequently reducing erosion and sediment yield, and enhancing soil retention in these areas. As the results indicate (Table 5), the highest and lowest rates of soil wastage and sediment yield are observed in urban areas and park, respectively, while the highest and lowest soil retention rates are found in forest lands and garden, respectively. The findings demonstrate that due to diversity in topography, rainfall, land use management, agricultural activities, deforestation, grazing, and other human actions, soil erosion and retention vary spatially across the llam watershed (Eniyew et al., 2021; Getu et al., 2022). Among these factors, the conditions of the watershed are largely dependent on land use distribution. Considering the land use pattern, the Ilam watershed is generally divided into northern, central, and southern sections. Forests dominate the northern section, while the central and southern sections are more influenced by built-up areas and agricultural activities. Examination of other parameters also confirms the differences between these three sections. The rainfall erosion map shows that the maximum occurs

Table 5. Attributable potential for soil retention, erosion, and sediment transport to each land use category

Landuse	Area	Soil retention potential		Erosion potential		Sediment transport potential	
	(ha)	Percentage	Tons per hectare	Percentage	Tons per hectare	Percentage	Tons per hectare
Dense Forest	5131	69	64.2	8	2.7	5	0.5
Sparse Forest	1752	20	26.1	5	3.45	4	0.59
Agriculture	1875	6	0.2	17	7.8	16	0.68
Orchard	238	0	0.36	1	0.96	1	0.3
Pasture	439.2	2	1.9	4	3.6	3	0.49
Urban Areas	3185	1	1.2	54	36.5	58	6.4
Park	35.8	0	0	0	0	0	0.1
Riverbed	202	1	0.6	4	3.78	4	0.7
Road Network	327	1	0	8	4.3	8	0.87

in the northern part and the minimum in the southern part. In terms of slope, the northern region has steep slopes, while more gentle slopes are seen in the central and southern parts. Therefore, the erosion status of the studied watershed results from various factors including landform, slope, rainfall erosion, and land use patterns. It is noteworthy that the central and southern sections, due to steep slopes, topography, and significant rainfall erosion, have a higher potential for soil loss and sediment yield compared to the northern areas. In other words, the northern region has a greater capacity for soil retention. Indeed, dense vegetation cover in the northern part is the primary factor creating these conditions, reducing the impact of other factors on increasing soil erosion and sediment yield in the northern areas. Moreover, dense forest cover is the main factor preventing erosion and soil degradation, providing the ES of soil retention in the northern and western parts of the Ilam watershed. Previous studies have also confirmed that vegetation cover is the most important factor in providing soil retention and acting as a barrier against soil erosion (Ahmadi Mirghaed et al., 2018; Yang et al., 2019; Kusi et al., 2020; Kretz et al., 2021). Overall, land use patterns are a significant factor in soil retention and the potential for erosion and sediment transport across the region, consistent with previous findings (Tamene et al., 2017; Vijith & Dodge-Wan, 2019; Aneseyee et al., 2020; Gashaw et al., 2021; Degife et al., 2021; Sadat et al., 2023; Sun et al., 2022; Tamire et al., 2022; Yang et al., 2023b). In general, and in confirmation of previous studies, the InVEST SDR model, despite some limitations such as not considering processes of gully, trench, and riverbank erosion and sedimentation, has high potential for modeling soil retention and estimating erosion and sediment. This model can facilitate the identification of focal areas for erosion and soil retention with very little input data and assess the effects of various factors, especially changes in land use. A study conducted in the Chardavol watershed of Ilam province utilized the RUSLE to evaluate the effects of land use change on soil erosion between 2005 and 2020. The results indicated a significant increase in average erosion rates from 13.23 tons/ha/year in 2005 to 20.13 tons/ha/ year in 2020, primarily attributed to changes in land use and vegetation cover (Gholami et al., 2024). Under this context, several practical measures can be implemented to mitigate erosion in the Ilam watershed:

- Forest conservation: Strict protection of existing forest cover, particularly in Sub-basins 2, 5, 6, 7, 8, and 11 where forests demonstrate high soil retention capacity (60% of total retention).
- Terracing and contour farming: Implementation on agricultural slopes, especially in Sub-basins 1 and 3 where agriculture covers 14% of the area but contributes disproportionately to sediment transport.
- Urban erosion control: Adoption of green infrastructure (permeable pavements, retention basins) in urban areas (24% of watershed) which show the highest erosion rates (36.5 tons/ha).

- Riparian buffers: Establishment along rivers (2% of area) to filter sediments before they reach water bodies.
- Conservation tillage: Promotion in agricultural areas to reduce soil disturbance and improve water infiltration.

The results of our study showed that the ecology and integrity of the Ilam watershed are primarily influenced by forest land uses in the northern part and urban areas in the central-southern part. In fact, urbanization and forest cover respectively play the main roles in maximizing the potential for erosion and sediment and soil retention. Despite the importance of forest ecosystems in controlling erosion and soil retention in the llam watershed, the destruction of forest ecosystems in the region, particularly in the Arghvan sub-basin (Code 8), under the pretext of development and construction, has led to intense land use and significant changes in the urban land use/cover patterns. Undoubtedly, these changes affect the supply and distribution of soil retention and seriously limit the value of ecosystem services, increasing ecosystem disservices such as erosion. To counteract the new patterns of land use change caused by continuous urban expansion and vegetation cover destruction, strict policies for the protection of forest lands, implementation of soil conservation projects, and ecological protection of forests, as well as effective engineering and biological measures to control erosion and sediment transport in the region, are recommended.

This study acknowledges certain limitations in methodology and data collection. For instance, while the InVEST SDR model provides valuable insights into sediment dynamics, its reliance on input data such as DEM resolution and land use classification may introduce uncertainties. Additionally, field validation of sediment transport estimates was constrained by logistical challenges.

#### 5. Conclusions

This study highlights that forested areas in the llam watershed retain approximately 60% of sediment while contributing only 13% to discharge. Conversely, urbanized and agricultural regions exhibit higher erosion potential, emphasizing the critical role of ecosystem services in soil conservation. The results of this study highlight the importance of ES in land evaluation and planning and emphasize the need to identify ES in the region and integrate them into land management as a useful strategy to enhance the efficiency of land management decisions. Accordingly, by establishing new management policies and providing optimal and practical solutions to reduce the consequences and negative impacts of land use on soil retention, the awareness of managers and decision-makers can be improved for adopting appropriate land management decisions. Additionally, considering the importance of forest ecosystems and their role in improving ES such as soil retention, enlightening public opinion and useful

educational programs for stakeholders, especially local communities, in recognizing the role of these ecosystems in enhancing the ES of the landscape of the Ilam watershed can be an effective step towards protecting these covers. Future research should focus on integrating highresolution temporal data to capture seasonal variations in sediment dynamics and exploring advanced modeling techniques to enhance accuracy in predicting erosion potential under varying climate scenarios.

The findings underscore the importance of incorporating ecosystem services into land management policies to mitigate erosion risks and promote sustainable development practices. Policymakers can leverage these insights to design targeted interventions for vulnerable regions.

## **Acknowledgements**

The authors of this article would like to thank Research Vice-Presidency of the faculty of Natural Resources and Earth Sciences and Shahrekord University for their supports.

#### **Disclosure statement**

The authors declare no conflict of interest.

## References

Ahmadi Mirghaed, F., Souri, B., Mohammadzadeh, M., Salmanmahiny, A., & Mirkarimi, S. H. (2018). Evaluation of the relationship between soil erosion and landscape metrics across Gorgan Watershed in northern Iran. Environmental Monitoring and Assessment, 190(11), Article 643.

https://doi.org/10.1007/s10661-018-7040-5

Aneseyee, A. B., Elias, E., Soromessa, T., & Feyisa, G. L. (2020). Land use/land cover change effect on soil erosion and sediment delivery in the Winike watershed, Omo Gibe Basin, Ethiopia. Science of the Total Environment, 728, Article 138776.

https://doi.org/10.1016/j.scitotenv.2020.138776

Azimi Sardari, M. R., Bazrafshan, O., Panagopoulos, T., & Sardooi, E. R. (2019). Modeling the impact of climate change and land use change scenarios on soil erosion at the Minab Dam Watershed. Sustainability, 11(12), Article 3353.

https://doi.org/10.3390/su11123353

Balabathina, V. N., Raju, R. P., Mulualem, W., & Tadele, G. (2020). Estimation of soil loss using remote sensing and GIS-based universal soil loss equation in northern catchment of Lake Tana Sub-basin, Upper Blue Nile Basin, Northwest Ethiopia. Environmental Systems Research, 9(1), 1-32.

https://doi.org/10.1186/s40068-020-00203-3

Bhattacharya, R. K., Chatterjee, N. D., & Das, K. (2024). Modelling of soil erosion susceptibility incorporating sediment connectivity and transport at landscape scale using integrated machine learning, InVEST-SDR and Fragstats. Journal of Environmental Management, 353, Article 120164.

https://doi.org/10.1016/j.jenvman.2024.120164

Borrelli, P., Robinson, D. A., Fleischer, L. R., Lugato, E., Ballabio, C., Alewell, C., Meusburger, K., Modugno, S., Schütt, B., Ferro, V., Bagarello, V., Van Oost, K., Montanarella, L., & Panagos, P., & Panagos, P. (2017). An assessment of the global impact of 21st century land use change on soil erosion. Nature Communications, 8(1), Article 2013.

https://doi.org/10.1038/s41467-017-02142-7

- Carucci, T., Whitehouse-Tedd, K., Yarnell, R. W., Collins, A., Fitzpatrick, F., Botha, A., & Santangeli, A. (2022). Ecosystem services and disservices associated with vultures: A systematic review and evidence assessment. Ecosystem Services, 56, Article 101447. https://doi.org/10.1016/j.ecoser.2022.101447
- Degife, A., Worku, H., & Gizaw, S. (2021). Environmental implications of soil erosion and sediment yield in Lake Hawassa watershed, south-central Ethiopia. Environmental Systems Research, 10(1), Article 28.

https://doi.org/10.1186/s40068-021-00232-6

da Cunha, E. R., Santos, C. A. G., da Silva, R. M., Panachuki, E., de Oliveira, P. T. S., de Souza Oliveira, N., & dos Santos Falcão, K. (2022). Assessment of current and future land use/cover changes in soil erosion in the Rio da Prata basin (Brazil). Science of the Total Environment, 818, Article 151811.

https://doi.org/10.1016/j.scitotenv.2021.151811

- Eniyew, S., Teshome, M., Sisay, E., & Bezabih, T. (2021). Integrating RUSLE model with remote sensing and GIS for evaluation soil erosion in Telkwonz Watershed, Northwestern Ethiopia. Remote Sensing Applications: Society and Environment, 24, Article 100623. https://doi.org/10.1016/j.rsase.2021.100623
- Gadisa, N., & Midega, T. (2021). Soil and water conservation measures in Ethiopia: Importance and adoption challenges. World Jol of Agri and Soil Science, 6(3), 1-7.

https://doi.org/10.33552/WJASS.2021.06.000636

Ganasri, B. P., & Ramesh, H. (2016). Assessment of soil erosion by RUSLE model using remote sensing and GIS - a case study of Nethravathi basin. Geoscience Frontiers, 7(6), 953-961. https://doi.org/10.1016/j.gsf.2015.10.007

- Gashaw, T., Tulu, T., & Argaw, M. (2018). Erosion risk assessment for prioritization of conservation measures in Geleda watershed, Blue Nile basin, Ethiopia. Environmental Systems Research, 6(1), 1-14. https://doi.org/10.1186/s40068-016-0078-x
- Gashaw, T., Bantider, A., Zeleke, G., Alamirew, T., Jemberu, W., Worqlul, A. W., Dile, Y. T., Bewket, W., Meshesha, D. T., Adem, A. A., & Addisu, S. (2021). Evaluating InVEST model for estimating soil loss and sediment transport in data scarce regions of the Abbay (Upper Blue Nile) Basin: Implications for land managers. Environmental Challenges, 5, Article 100381. https://doi.org/10.1016/j.envc.2021.100381
- Getu, L. A., Nagy, A., & Addis, H. K. (2022). Soil loss estimation and severity mapping using the RUSLE model and GIS in Megech watershed, Ethiopia. Environmental Challenges, 8, Article 100560. https://doi.org/10.1016/j.envc.2022.100560
- Gholami, L., Khaledi Darvishan, A., Derakhti, S., & Kiani Harchegani, M. (2024). Effects evaluation of land use change on soil erosion using the RUSLE model in the Chardavol watershed, Ilam. Journal of Water Management and Soil Erosion, 18(65), 1–14.
- Guo, B., Yang, F., Fan, J., & Lu, Y. (2022). The changes of spatiotemporal pattern of rocky desertification and its dominant driving factors in typical karst mountainous areas under the background of global change. Remote Sensing, 14(10), Article 2351. https://doi.org/10.3390/rs14102351
- Hamel, P., Chaplin-Kramer, R., Sim, S., & Mueller, C. (2015). A new approach to modelling the sediment retention service (InVEST 3.0): Case study of the Cape Fear catchment, North Carolina, USA. Science of the Total Environment, 524-525, 166-177. https://doi.org/10.1016/j.scitotenv.2015.04.027
- Kusi, K. K., Khattabi, A., Mhammdi, N., & Lahssini, S (2020). Prospective evaluation of the impact of land use change on ecosystem services in the Ourika watershed, Morocco. Land Use

- Policy, 97, Article 104796.
- https://doi.org/10.1016/j.landusepol.2020.104796
- Kretz, L., Koll, K., Seele-Dilbat, C., van der Plas, F., Weigelt, A., & Wirth, C. (2021). Plant structural diversity alters sediment retention on and underneath herbaceous vegetation in a flume experiment. *PLoS One*, 16(3), Article e0248320.
  - https://doi.org/10.1371/journal.pone.0248320
- Liu, Y., Lü, Y., Zhao, M., & Fu, B. (2023). Integrative analysis of biodiversity, ecosystem services, and ecological vulnerability can facilitate improved spatial representation of nature reserves. *Science of the Total Environment*, 879, Article 163096. https://doi.org/10.1016/j.scitotenv.2023.163096
- Liu, W., Shi, C., Ma, Y., Li, H., & Ma, X. (2021). Land use and land cover change-induced changes of sediment connectivity and their effects on sediment yield in a catchment on the Loess Plateau in China. *Catena*, 207, Article 105688. https://doi.org/10.1016/j.catena.2021.105688
- Mazigh, N., Taleb, A., El Bilali, A., & Ballah, A. (2022). The effect of erosion control practices on the vulnerability of soil degradation in Oued EL Malleh catchment using the USLE model integrated into GIS, Morocco. *Trends in Sciences*, *19*(2), 2059–2059. https://doi.org/10.48048/tis.2022.2059
- Millennium Ecosystem Assessment. (2005). *Ecosystems and human well-being*. Island Press.
- Moges, D. M., & Bhat, H. G. (2017). Integration of geospatial technologies with RUSLE for analysis of land use/cover change impact on soil erosion: Case study in Rib watershed, northwestern highland Ethiopia. *Environmental Earth Sciences*, 76, 1–14. https://doi.org/10.1007/s12665-017-7109-4
- Ougougdal, H. A., Khebiza, M. Y., Messouli, M., & Bounoua, L. (2020). Delineation of vulnerable areas to water erosion in a mountain region using SDR-InVEST model: A case study of the Ourika watershed, Morocco. *Scientific African*, *10*, Article e00646. https://doi.org/10.1016/j.sciaf.2020.e00646
- Paudel, S., & States, S. (2023). Urban green spaces and sustainability: Exploring the ecosystem services and disservices of grassy lawns versus floral meadows. *Urban Forestry & Urban Greening*, 84, Article 127932. https://doi.org/10.1016/j.ufug.2023.127932
- Potschin-Young, M., Czúcz, B., Liquete, C., Maes, J., Rusch, G. M., & Haines-Young, R. (2017). Intermediate ecosystem services: An empty concept? *Ecosystem Services*, *27*(Part A), 124–126. https://doi.org/10.1016/j.ecoser.2017.09.001
- Sadeghi, S. H. R. (1993). An overview of the Modified Pacific Southwest Inter-Agency Committee model for estimating soil erosion in Iran. *Journal of Soil and Water Conservation*, 48(4), 345–350.
- Srichaichana, J., Trisurat, Y., & Ongsomwang, S. (2020). Land use and land cover scenarios for optimum water yield and sediment retention ecosystem services in Klong U-Tapao Watershed, Songkhla Thailand. Sustainability, 11(10), 1–22. https://doi.org/10.3390/su11102895
- Sharp, R., Tallis, H. T., Ricketts, T., Guerry, A. D., Wood, S. A., Chaplin-Kramer, R., Nelson, E., et al. (2020). *InVEST* 3.8.9 *user's guide*. The Natural Capital Project, Stanford University, University of Minnesota, The Nature Conservancy, and World Wildlife Fund.

- Sun, Y., Liu, D., & Wang, P. (2022). Urban simulation incorporating coordination relationships of multiple ecosystem services. Sustainable Cities and Society, 76, Article 103432. https://doi.org/10.1016/j.scs.2021.103432
- Tamene, L., Adimassu, Z., Aynekulu, E., & Yaekob, T. (2017). Estimating landscape susceptibility to soil erosion using a GIS-based approach in Northern Ethiopia. *International Soil and Water Conservation Research*, *5*(3), 221–230. https://doi.org/10.1016/j.iswcr.2017.05.002
- Tamire, C., Elias, E., & Argaw, M. (2022). Spatiotemporal dynamics of soil loss and sediment transport in Upper Bilate River Catchment (UBRC), Central Rift Valley of Ethiopia. *Heliyon*, 8(11), Article e11220. https://doi.org/10.1016/j.heliyon.2022.e11220
- Yang, Y., Zhang, D., Nan, Y., Liu, Z., & Zheng, W. (2019). Modeling urban expansion in the transnational area of Changbai Mountain: A scenario analysis based on the zoned Land Use Scenario Dynamics-urban model. Sustainable Cities and Society, 50, Article 101622. https://doi.org/10.1016/j.scs.2019.101622
- Yang, W., Bai, Y., Ali, M., Huang, Z., Yang, Z., & Zhou, Y. (2023a). Quantifying the difference between supply and demand of ecosystem services at different spatial-temporal scales: A case study of the Taihu Lake Basin. *Circular Agricultural Systems*, 3, Article 5. https://doi.org/10.48130/CAS-2023-0005
- Yang, J., Zhai, D. L., Fang, Z., Alatalo, J. M., Yao, Z., Yang, W., Su, Y., Bai, Y., Zhao, G., & Xu, J. (2023b). Changes in and driving forces of ecosystem services in tropical southwestern China. *Ecological Indicators*, *149*, Article 110180.
  - https://doi.org/10.1016/j.ecolind.2023.110180
- Yohannes, H., Soromessa, T., Argaw, M., & Dewan, A. (2021). Impact of landscape pattern changes on hydrological ecosystem services in the Beressa watershed of the Blue Nile Basin in Ethiopia. *Science of the Total Environment, 793*, Article 148559. https://doi.org/10.1016/j.scitotenv.2021.148559
- Vigiak, O., Borselli, L., Newham, L. T. H., McInnes, J., & Roberts, A. M. (2012). Comparison of conceptual landscape metrics to define hillslope-scale sediment delivery ratio. *Geomorphology*, *138*, 74–88. https://doi.org/10.1016/j.geomorph.2011.08.026
- Vijith, H., & Dodge-Wan, D. (2019). Modelling terrain erosion susceptibility of logged and regenerated forested region in northern Borneo through the Analytical Hierarchy Process (AHP) and GIS techniques. *Geoenvironmental Disasters*, 6(1), Article 8. https://doi.org/10.1186/s40677-019-0124-x
- Zakeri, A., Fadaei, R., & Mohammadi, A. (2015). Evaluation of soil losses and sediment yield using modified PSIAC model in a watershed. *Journal of Water and Soil Conservation*, *22*(1), 85–92.
- Zhou, M., Deng, J., Lin, Y., Belete, M., Wang, K., Comber, A., Huang, L., & Gan, M. (2019). Identifying the effects of land use change on sediment transport: Integrating sediment source and sediment delivery in the Qiantang River Basin, China. *Science of the Total Environment*, 686, 38–49. https://doi.org/10.1016/j.scitotenv.2019.05.336
- Zhao, J., Shao, Z., Xia, C., Fang, K., Chen, R., & Zhou, J. (2022). Ecosystem services assessment based on land use simulation: A case study in the Heihe River Basin, China. *Ecological Indicators*, *143*, Article 109402.
  - https://doi.org/10.1016/j.ecolind.2022.109402